Journal of Young Pharmacists, 2026; 18(3):840-849.
https://www.jyoungpharm.org

Original Article

Structural and Conformational Landscape of CDK4: The Basis for Next-Generation Kinase Therapeutics

Rashed Mohammed Alghamdi*

Department of Laboratory Medicine, Faculty of Applied College, Al-Baha University, SAUDI ARABIA.

ABSTRACT

Background: CDK4 (303 amino acids) is a serine/threonine kinase that regulates the G1-S transition and which is dysregulated in oncogenesis, and thus is an important target of kinase therapeutics. Structural Profiling aids in understanding conformational stability, inhibitor binding and resistance. **Objectives:** To conduct a brief *in silico* analysis of the kinase domain of CDK4 (Cyclin-dependent kinase 4, focusing on structure and conformational changes to guide therapeutics and structure-based drug design. **Materials and Methods:** The amino acid composition and the distribution of molecular weights of the 303-aa sequence of CDK4 was evaluated. Physico-chemical variability was analyzed using ProtScale sliding windows analysis. The structural quality was checked by Ramachandran (φ/ψ) analysis and G-factor assessment. Geometric criteria, Ca-Ca (alpha carbon-alpha carbon) distances were applied to Secondary structure, topology, β-bulges, β-turns and γ-turns were predicted. **Results:** Leucine was the most abundant amino acid (~9%), followed by a balanced distribution of hydrophobic and polar residues, with a balance of hydrophobic/polar content; more than 90% of the residues had G-factors near zero, and no residues were disallowed. The predicted architecture consisted of 13 α-helices and 8 β-strands, which are typical of the α/β kinase fold, along with 23 β-turns, 2 γ-turns, and several antiparallel β-bulges. **Conclusion:** CDK4 demonstrates a stable α/β kinetic framework in which the stereochemistry is reliable and defined by distinct conformational motifs, which enables the rational development of next generation CDK4 kinase therapeutics.

Keywords: Cyclin-Dependent Kinase 4, Conformational Analysis, Kinase Therapeutics, Molecular Topology, Protein Structural Analysis, Ramachandran Plot, Stereochemical Validation, Secondary Structure Prediction, Targeted Cancer Therapy.

Correspondence:
Dr. Rashed Mohammed Alghamdi
Department of Laboratory Medicine, Faculty of Applied College, Al-Baha University, SAUDI ARABIA.
Email: rmalghamdi@bu.edu.sa; rashed053660518@gmail.com

Received: 21-04-2026;
Revised: 09-06-2026;
Accepted: 14-08-2026.

INTRODUCTION

Proteins are basic macromolecules that regulate almost all biological processes such as catalysis, signal transduction, transport and structural functions. Functional properties of a protein are an inherent consequence of its amino acid sequence and thus its three-dimensional structure (3D) (Morris *et al.*, 2022). The link between sequence, structure and function continues to be an important goal of structural bioinformatics and molecular biology research (Jumper *et al.*, 2021; Thornton *et al.*, 2021; Thornton *et al.*, 2021). The primary sequence features, secondary structure elements and the stereochemical quality of the protein are important characteristics that can be analysed by computation and help to give insight into protein stability, folding and biological activity.

In the present study, a protein with 303 amino acids is focused upon. The amino acid composition and molecular weight distribution were performed as preliminary steps in the evaluation of primary structure. The properties of the protein can also be affected by changes in the composition of residues; these can include hydrophobicity, charge distribution and conformational flexibility, all of which can play a role in protein folding and stability (Kyte and Doolittle, 1982; Dill and MacCallum, 2012). The conformationally flexible residues (glycine) and the conformationally constraining residues (proline) are especially important to consider as they represent a type of residue that is distributed across the structure.

Secondary structure prediction of the protein revealed the presence of several α-helices and β-strands with turns and loops connecting them. Other structural elements that help maintain compact protein folding are the β-turns and γ-turns that reverse the direction of the polypeptide chain and stabilize tertiary interactions (Imai *et al.*, 2005). Beta bulges and antiparallel β-sheet configurations also suggest hydrogen-bonded networks that are organized and play a crucial role in the structure's integrity. All of them are similar to some of the emerging paradigms of

DOI: 10.5530/jyp.20260334

protein architecture: stable folds are made from recurring motifs (Branden and Tooze, 1999).

Stereochemical quality assessment was carried out by Ramachandran plot analysis by calculating dihedral angles (φ and ψ) of the backbone atoms to check the conformation feasibility. Backbone geometry and structural refinement (Ramachandran *et al*., 1963; Lovell *et al*., 2003) are good if high percentage of residues are in favored regions. Also, G-factor analysis gives quantitative assessment of dihedral angle distributions and covalent geometry which makes it possible to detect conformation uncharacteristics or strained geometries. Suitable values for the G-factor indicate that the structure modeled is in good accord with the stereochemical parameters (Engh *et al*., 1991).

Topology analysis also shows the spatial arrangement of helices and strands and provides insight into the global fold organisation. The use of the sequence-based analysis, secondary structure mapping, Ramachandran statistics and geometric validation gives a comprehensive structural framework. This computational characterization that integrates the protein is necessary in order to predict protein function, guide mutational studies and support drug design efforts (Schlick *et al*., 2010; Hou *et al*., 2003).

The field of protein structural biology has been transformed by the use of AI-driven structure prediction, notably deep learning methods like AlphaFold for accurately modelling protein structures *in silico* (Chen *et al*., 2024; Jumper *et al*., 2021). However, a thorough validation with stereochemical metrics and structural analysis tools is still essential to assure the structural reliability. Hence, the detailed structural assessment based on detailed compositional analysis, identification of the secondary structure and conformational validation are the backbone in understanding the behavior of protein at the molecular level.

MATERIALS AND METHODS

Design a sequence retrieval and Primary structure analysis

In this study, the protein sequence used is of 303 amino acids. Primary structure was retrieved using FASTA (Fast-All sequence format) format and then amino acid composition analysis was performed. The residues frequency, percentage composition, and molecular weight were computed from the sequence. Amino acid distribution and physico-chemical profiling were used to evaluate distribution of residues, hydrophobicity distribution and compositional bias.

The Kyte Doolittle algorithm was used for hydropathic analysis to assess the hydrophobic/hydrophilic regions of polypeptide chain (Kyte and Doolittle, 1982). The variation of molecular weights along the sequence has been determined with the aid of ProtScale, a tool for analysis of the physico-chemical properties at each position of the sequence (Gasteiger *et al*., 2005).

Secondary Structure Prediction and Modeling

The secondary structure elements such as α-helices, β-strands, β-turns and γ-turns were predicted with the help of structure prediction algorithms embedded in bioinformatics platform (PSIPRED). Hydrogen bonding patterns along the backbone and statistical propensity scales (Chou and Fasman, 1974; Jones, 1999) were used for identifying helices and strands.

Topology diagrams were created to represent the spatial organization of the secondary structure and the connections between them. The presence of β-bulges in the beta-structure and anti/parallel interactions between β-strands were confirmed by deviations in the alignment of the strands and hydrogen-bond geometry. The amphipathicity and the orientation of the side chains in an α-helix were evaluated by helical wheel projections.

Homology modeling and deep learning based structure prediction methods were used for three-Dimensional (3D) structure modeling. For proteins of structural homology, template-based modeling was performed, and for high confidence predictions of structurally similar proteins, such as AlphaFold (Jumper *et al*., 2021).

Molecular graphics software was used to view and analyse structure to observe folding patterns, domain organization, and residue packing.

A Ramachandran Plot Analysis and a Geometric Assessment and Assessment of the G-Factor

Stereochemical quality of backbone was assessed by the Ramachandran plot analysis based on the dihedral angles (phi (φ) and psi (ψ)) (Ramachandran *et al*., 1963). The percentage of residues in most favored, additionally allowed, generously allowed and disallowed regions was determined. Backbone geometry is acceptable if the backbone regions are highly occupied (Lovell *et al*., 2003).

The quantification of the deviations in dihedral angles and covalent geometry was done using G-factor analysis. The following parameters were analyzed: phi-psi distribution, chi-angle distribution, bond length and bond angle. For the purpose of this investigation, the structural validation criteria outlined in Laskowski *et al* (1993) were followed by assigning a g-factor value of less than -0.5 as unusual and less than -1.0 as highly unusual.

Analyze the structure of a piece for motifs and turns

Beta turns and gamma turns were found according to geometric criteria on the basis of the distance between the Cα atoms and the geometric constraints of the dihedral angles of the backbone. The classification of turns were according to the conformational categories known (Hutchinson and Thornton, 1994). Motif detection was carried out to find out local folding patterns which are involved in tertiary structure organisation in a compact form.

RESULTS

Primary Structure and Physico-chemical Analysis

The protein analyzed is called CDK4, and contains 303 amino acids (Figure 1A). The sequence is shown from the N-terminus to C-terminus with residue numbering clearly indicated, which is a complete polypeptide.

The molecular weight dispersity of the different amino acids is shown in the Figure 1B. The molecular weight of tryptophan and tyrosine is the highest and it is the lowest in the case of glycine. This distribution is the anticipated physico-chemical range of residue types.

The amino acid composition analysis (Figure 1C) shows that the most common residues are leucine (~9%), alanine, and serine, with lower frequencies of tryptophan and cysteine. The composition profile shows that the compound is a balanced distribution of polar, nonpolar and charged residues.

The molecular weight variation along the sequence (Figure 1D) shows moderate variations and reveals local variations in the mass density of the residues of the molecule. Likewise, the amino acid composition profile of the ProtScale (Figure 1E) identifies compositional enrichment and depletion regions, indicating structurally and/or functionally different parts of the protein.

Structural Validation and Secondary Structure Prediction

The Ramachandran plot (Figure 2A) reveals that most of the residues fall into the energetically favorable regions of backbone dihedral angles, φ and ψ. The quantitative analysis (Figure 2B) shows that more than 90% of the residues are in the most favored regions, and only a small number of residues are found in generously allowed regions and no residue is found in disallowed regions. It is an indication of the high stereochemical quality of the predicted model. The stereochemical parameters are acceptable and the average for the entire G-factor is near zero (Figure 2C), which means that there is no significant structural strain.

The topology diagram (Figure 2D) shows a mixed α/β fold composed of several helices, as well as several β-strands, interspersed with loop regions. Structurally complex architecture is predicted by the secondary structure map (Figure 2E), which reveals thirteen α-helices (H1-H13), some β-strands, β-turns, and β-hairpins throughout the sequence (Table 1).

β-Bulges and Helical Wheel Analysis

A few antiparallel β-bulges were discovered (Figure 3A), where certain residue pair distortions exist in β-strands. According to their classification (Figure 3B), they have both the classic and C1-type antiparallel β-bulges based on the φ/ψ distribution and residue interaction (Tables 2 and 3).

The helical wheel projections (Figure 3C) for the predicted α-helices show different patterns of residue segregation. The helices of many helices exhibit amphipathic structure, with hydrophobic residues on one side, and polar/charged residues on the other, indicating possible functional interfaces (Table 4).

β-Turn and γ-Turn Analysis

There were 23 total β-turn motifs found throughout the sequence (Figure 4A), with Types I, II, IV and VIII. The Cα-Cα distance is ca. 5.0-6.8Å, consistent with the typical distances of β-turns. Moreover, the presence of two γ-turns was observed, one of which was an inverse turn (Figure 4B). They have similar backbone turn angles (φ/ψ) and Cα-Cα distances (~5.3-5.7 Å) which are within the normal range for backbone structure, suggesting the presence of tight backbone turns that afford local folding stability (Tables 5 and 6).

DISCUSSION

The detailed structure determination of the 303-residue protein offers valuable clues to its folding structure, stability and possibly functional attributes. A combination of the primary sequence analysis, secondary structure prediction, topology mapping and stereochemical validation provides a coherent interpretation of the structure, consistent with known principles of protein architecture (Tsuboyama *et al.*, 2023; Zhao *et al.*, 2025).

The amino acid composition analysis showed the even distribution of polar, charged and hydrophobic residues. Of special note, are the multiple glycine and proline residues (Skrbic *et al.*, 2024; Desantis *et al.*, 2022). As a result, glycine (Gly) has no side chain which increases conformational flexibility and proline (Pro) has a rigid side chain and tends to favor the formation of turns. This is the expected type of distribution that can be seen in the abundance of β-turns and γ-turns in the structure. The conformational features of these compositions are all in line with known correlations between residue type and preferred

Table 1: Beta hairpins.

Sl. No.	Strand 1			Strand 2			Hairpin Class
	Start	End	Length	Start	End	Length	
1.	Glu7	Gly15	9	Gly18	Arg24	7	2:21
2.	Gly18	Arg24	7	Phe31	Pro40	10	4:6
3.	Leu74	Arg82	9	Glu86	Glu94	9	2:4
4.	Ile146	Val148	3	Val154	Leu156	3	3:5

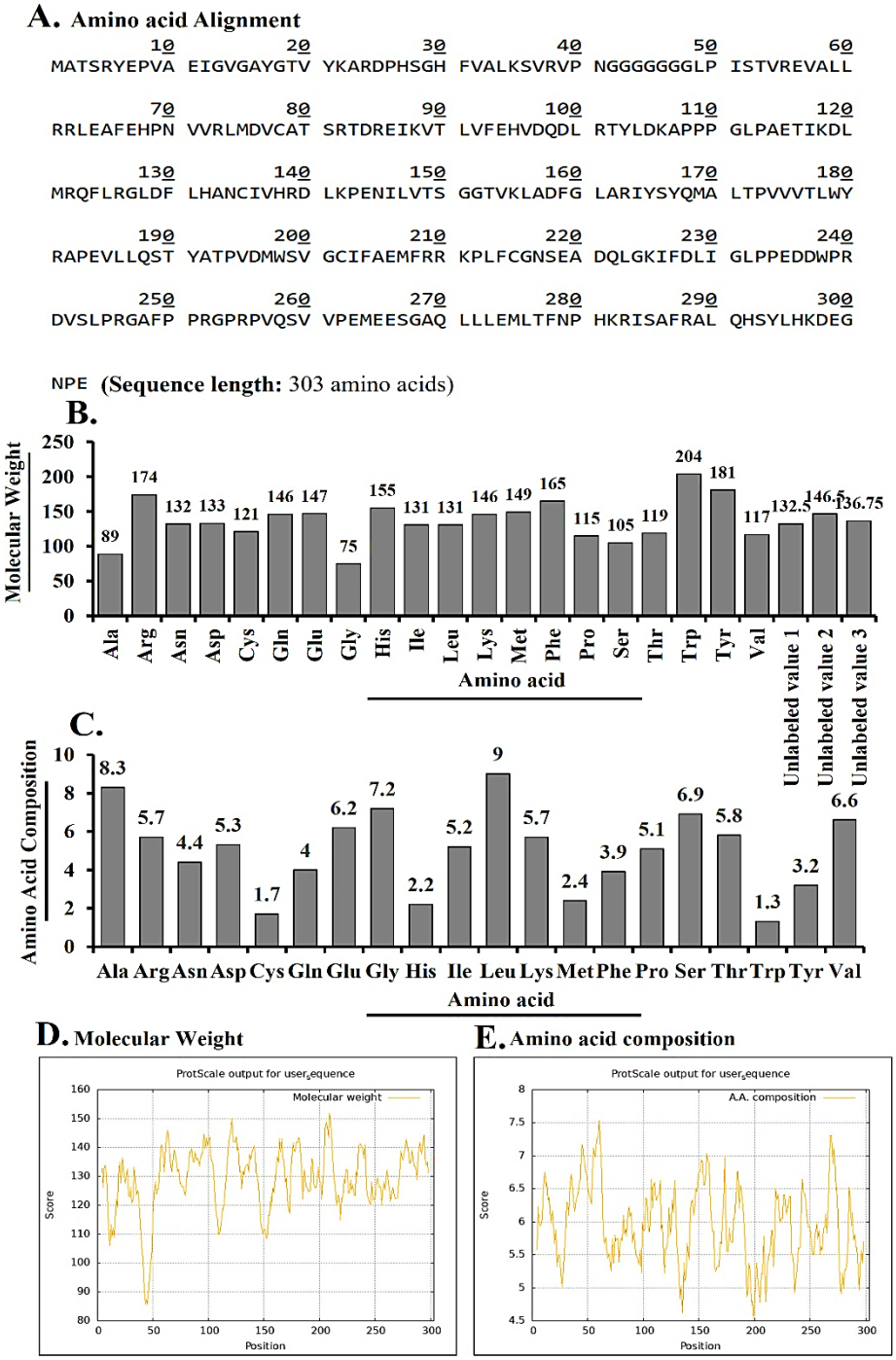

Figure 1: The primary structure and physiochemical profiling of 303-aa CDK4 protein. (A) Sequence; (B) Molecular weight; (C) Amino acid composition; (D) Residue molecular weight profile; (E) ProtScale profile.

conformation of the backbone (Chou and Fasman, 1974; Dill and MacCallum, 2012).

The hydropathic profiling indicates that there are alternating hydrophobic and hydrophilic regions, which are suggestive of α-helices and β-strands that are amphipathic. The amphipathicity is a typical protein structure characteristic that is found in the globular proteins which is essential for proper core packing and solvent exposure pattern (Kyte and Doolittle, 1982).

Secondary structure analysis showed a number of α-helices connected by β-strands and loop regions creating a compact and organized fold. The occurrence of antiparallel β-sheets and β-bulges indicate stable hydrogen-bonding networks. The beta bulges may be important for subtle structural deviations that allow the strands to align precisely and for functional formation of the surface (Richardson and Richardson, 2002; Wang *et al.*, 2020).

The topology is clearly folded and the helices are well organized as if in a domain-like fashion. The chain reversals are achieved by the recurrent structural motifs, β-turns and γ-turns, which help to increase the tertiary packing efficiency. The regions with high turn values tend to be involved in molecular recognition or in the formation of an active site (Hutchinson and Thornton, 1994). Helical wheel projections show amphipathic helices and segregation of hydrophobic and polar residues, which are good for the stable core formation and possible interaction interfaces. Functional protein domains that recognize a ligand or protein-protein interactions tend to have such amphipathic helices (Branden and Tooze, 1999; Gimenez-Andres *et al.*, 2018).

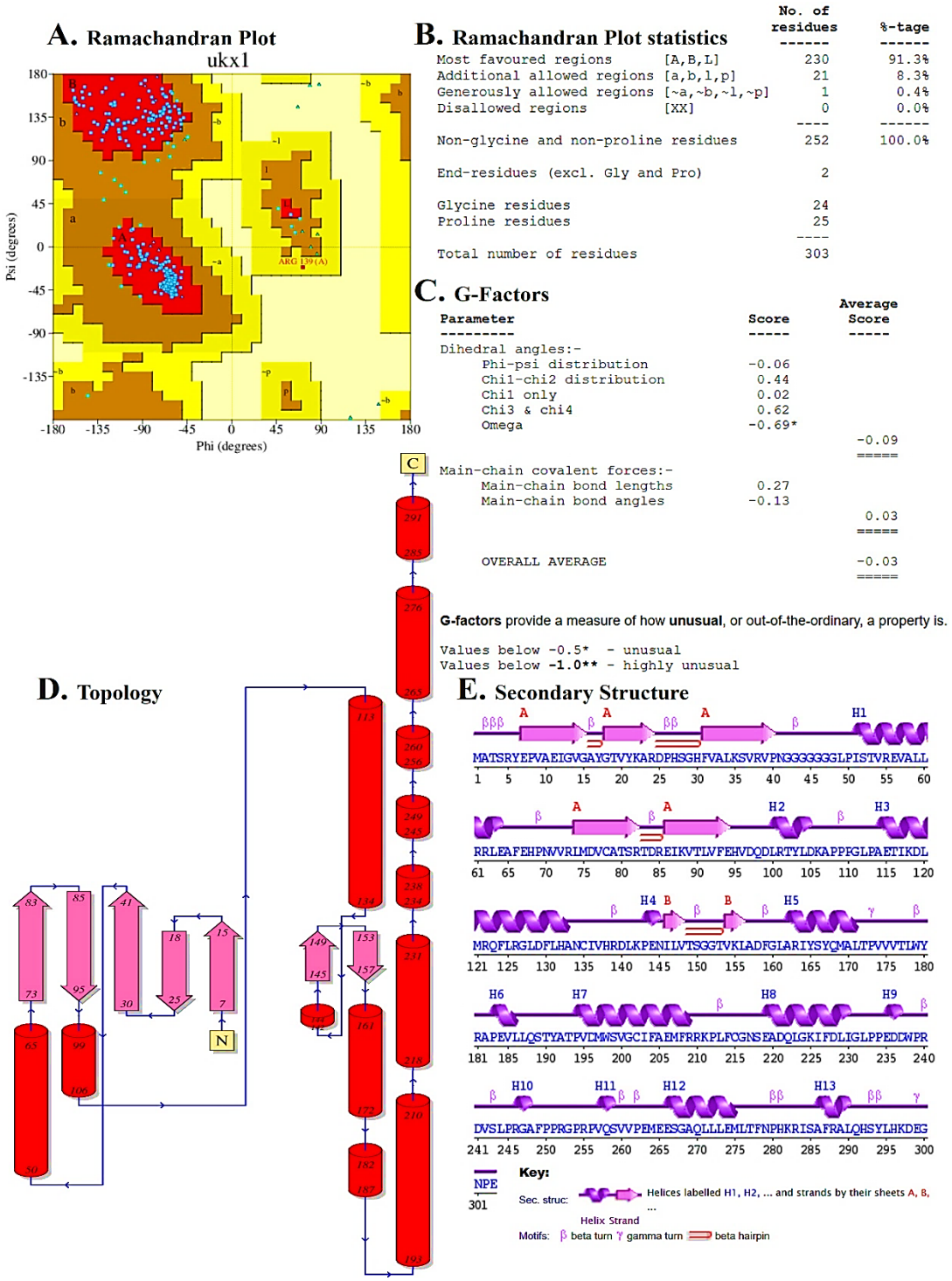

Figure 2: The structure and secondary structure of CDK4 were validated. (A) Ramachandran plot. (B) Ramachandran statistics. (C) G-factor analysis. (D) Structure of α-helices and β-strands, topology diagram. (E) Secondary structure predicted: α-helices (H1-H13), β-strands, β-turns and β-hairpins.

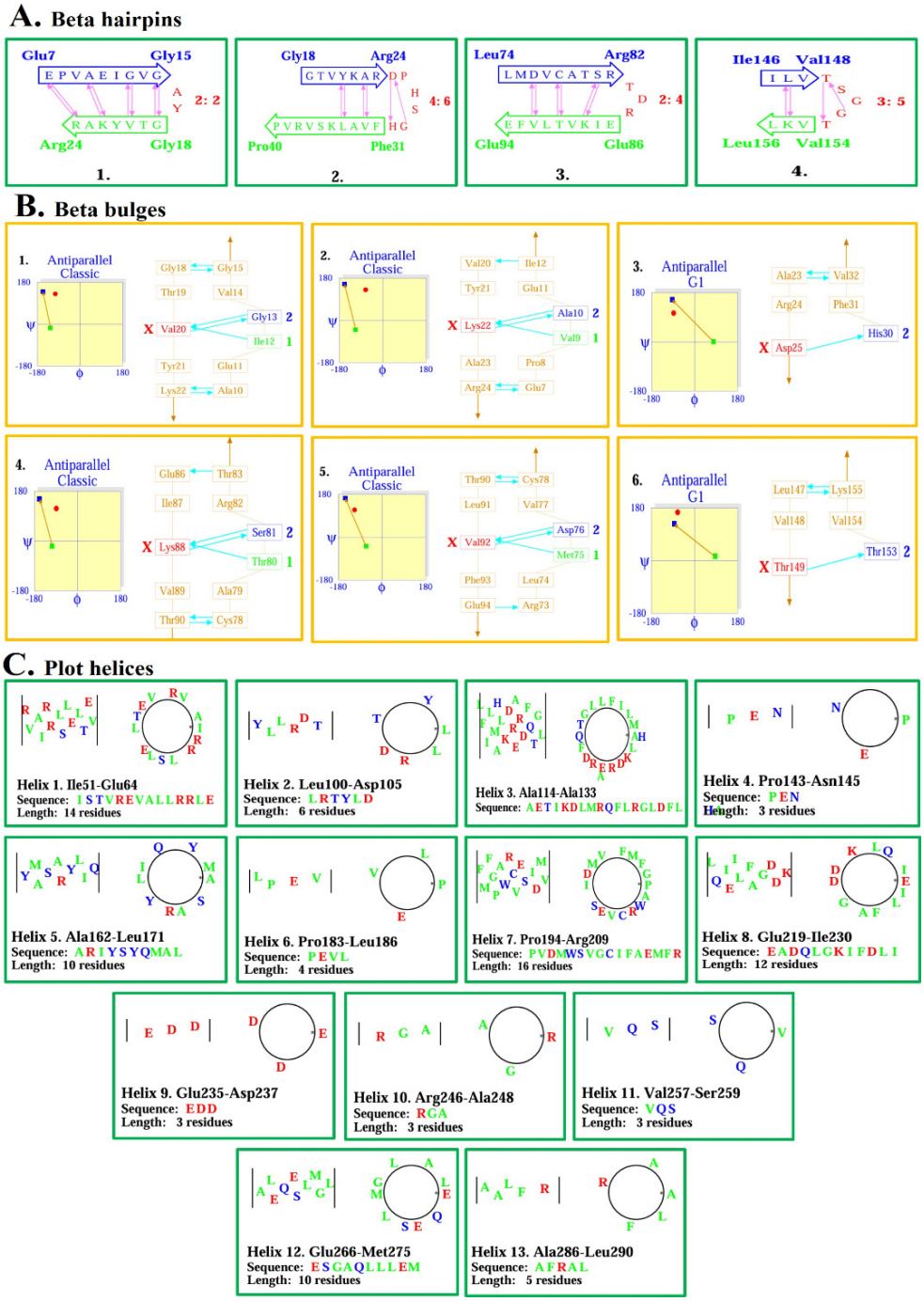

Figure 3: β-Bulges and helical wheel projections. (A) Beta bulge motifs that are antiparallel to each other. (B) β-Bulge classes and Ramachandran distributions. (C) The helical wheel projection of α-helices (H1-H13) displaying arrangement of residues and amphipathicity.

The majority of the residues are found in the most favored regions and there is no appreciable density in the disallowed regions in the Ramachandran plot statistics. This distribution is good for good backbone geometry and good stereochemical refinement. The high proportion of residues in favourable regions is a good sign of the reliability of the model, as per current structural validation standards (Ho *et al.*, 2003; Lovell *et al.*, 2003).

The G-factor analysis also backs up structural integrity. A value near to zero for phi-psi and dihedral angles for the side-chain shows that these angles differ little from ideal geometry. There is some variation in the omega angles, however, it is within reasonable limits. G-factor is a high-level measure that can be used to identify unusual conformations and structural strain (Laskowski *et al.*, 1993; Yasuda *et al.*, 2022).

There are several β-turns and γ-turns identified which indicate dynamic regions that could be responsible for conformational adaptability. These flexible regions frequently serve as binding sites for substrates, switch their conformation or are involved in binding regulatory molecules. Furthermore, the presence of organised elements of secondary structure with flexible loops that allow for adaptation with respect to function are a hallmark of globular proteins, that are structurally stable and flexible (de Brevern *et al*., 2016; Perczel *et al*., 1996).

The reliability of computational models has been drastically enhanced in recent years, thanks to new developments in structure prediction via AI, such as AlphaFold (Jumper *et al*., 2021). But, the validation of the model by stereochemical analysis (Ramachandran) and G-factor is still necessary to ensure the quality of the model. In this study, the correlation of the predicted secondary structure, the topology organization and stereochemical validation increases the confidence in the structural interpretation.

Table 2: Beta bulges.

Sl. No.	Bulge type	Res X	Res 1	Res 2
*1.	Antiparallel classic	Val20A	Ile12A	Gly13A
*2.	Antiparallel classic	Lys22A	Val9A	Ala10A
*3.	Antiparallel G1	Asp25A	Gly29A	His30A
*4.	Antiparallel classic	Lys88A	Thr80A	Ser81A
5.	Antiparallel classic	Val92A	Met75A	Asp76A
6.	Antiparallel G1	Thr149A	Gly152A	Thr153A

Table 3: Beta strands.

Sl. No.	Start	End	Sheet	No. residues	Edge	Sequence
1.	Glu7	Gly15	A	9	Yes	EPVAEIGVG
2.	Gly18	Arg24	A	7	No	GTVYKAR
3.	Phe31	Pro40	A	10	No	FVALKSVRVP
4.	Leu74	Arg82	A	9	Yes	LMDVCATSR
5.	Glu86	Glu94	A	9	No	EIKVTLVFE
6.	Ile146	Val148	B	3	Yes	ILV
7.	Val154	Leu156	B	3	Yes	VKL

Number of strands in chain A: 7.

Table 4: Helices.

Sl. No.	Start	End	Type	No. Residues	Length	Unit Rise	Residues per turn	Pitch	Deviation from ideal	Sequences
*1.	Ile51	Glu64	H	14	21.77	1.51	3.60	5.44	5.3	ISTVREVALLRRLE
*2.	Leu100	Asp105	H	6	9.16	1.45	3.49	5.06	4.6	LRTYLD
*3.	Ala114	Ala133	H	20	30.20	1.48	3.68	5.44	10.5	AETIKDLMRQFLRGLDFLHA
*4.	Pro143	Asn145	G	3	-	-	-	-	-	PEN
5.	Ala162	Leu171	H	10	15.57	1.54	3.48	5.35	21.6	ARIYSYQMAL
6.	Pro183	Leu186	H	4	6.40	1.48	3.72	5.49	38.6	PEVL
7.	Pro194	Arg209	H	16	24.58	1.53	3.50	5.35	12.5	PVDMWSVGCIFAEMFR
8.	Glu219	Ile230	H	12	17.37	1.46	3.67	5.35	13.9	EADQLGKIFDLI
9.	Glu235	Asp237	G	3	-	-	-	-	-	EDD
10.	Arg246	Ala248	G	3	-	-	-	-	-	RGA
11.	Val257	Ser259	G	3	-	-	-	-	-	VQS
12.	Glu266	Met275	H	10	15.43	1.51	3.54	5.35	2.6	ESGAQLLLEM
13.	Ala286	Leu290	H	5	8.05	1.52	3.53	5.37	20.0	AFRAL

Number of helices in chain A: 13

* Asterisked motifs correspond to those illustrated in the motif plots at the top of the page.

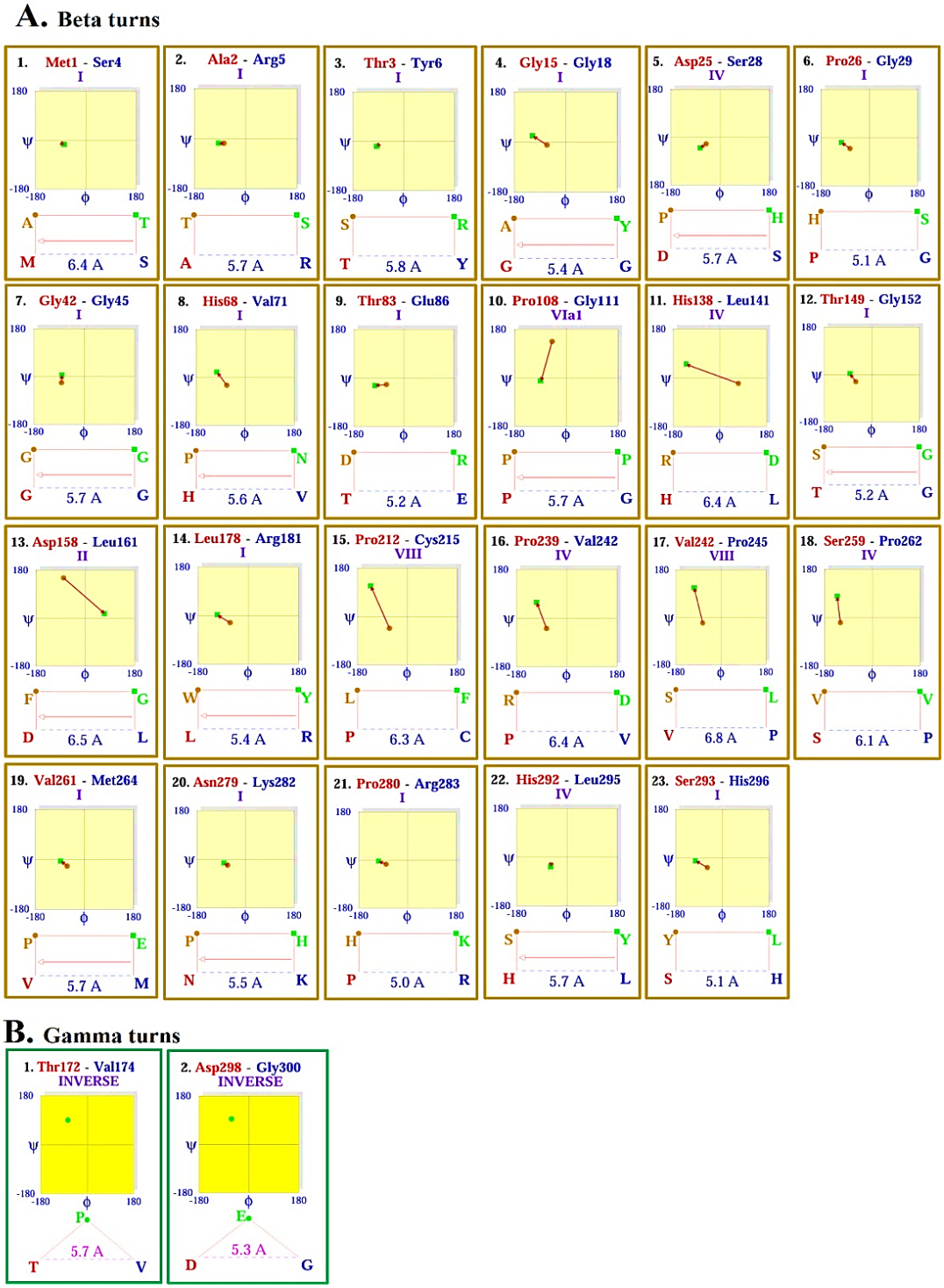

Figure 4: Characterization of β-turn and γ-turn (Figure). (A) β-turns labeled with type (I, II, IV, VIII, etc.) and distances (Å) between the two residues separated by the turn. (B) γ-turns (including inverse) with φ/ψ distributions and Cα-Cα distances.

The overall protein has the properties of a well folded globular protein with stable secondary structural components, organized topology and high stereochemical quality. The helices and strands distribution, together with the good Ramachandran statistics and the good G-factors, demonstrates in evidence structural robustness. Amphipathic helices and turn-rich regions may suggest functional specialization, which might have binding and/or catalytic functions.

Molecular dynamics simulations, ligand docking studies, and experimental validation (such as X-ray crystallography or

Table 5: Beta turns.

Sl. No.	Turns	Sequences*	Turn Type	Residue i+1			Residue i+2			I to i+3 CA-Dist	H-bond
				Phi	Psi	Chi1	Phi	Psi	Chi1		
*1.	Met1-Ser4	MATS	I	-80.8	-15.1	-	-75.6	-17.2	36.2	6.4	No
*2.	Ala2-Arg5	ATSR	I	-75.6	-17.2	36.2	-92.9	-18.6	53.7	5.7	Yes
*3.	Thr3-Tyr6	TSRY	I	-92.9	-18.6	53.7	-95.0	-21.3	-178.6	5.8	Yes
*4.	Gly15-Gly18	GAYG	I	-64.6	-11.3	-	-113.3	20.4	-54.7	5.4	No
*5.	Asp25-Ser28	DPHS	IV	-50.5	-25.9	-23.0	-71.3	-42.0	-67.3	5.7	No
6.	Pro26-Gly29	PHSG	I	-71.3	-42.0	-67.3	-102.3	-19.5	66.8	5.1	Yes
7.	Gly42-Gly45	CGGG	I	-80.6	-24.2	-	-78.7	4.6	-	5.7	No
8.	His68-Val71	HPNV	I	-66.5	-30.1	20.3	-101.3	17.2	-59.7	5.6	No
9.	Thr83-Glu86	TDRE	I	-62.6	-24.8	-62.0	-102.5	-28.7	-62.8	5.2	Yes
10.	Pro108-Gly111	PPPG	Vla1	-48.4	134.4	-23.9	-87.3	-13.3	30.0	5.7	No
11.	His138-Leu141	HRDL	IV	71.8	-21.3	-52.1	-128.9	49.0	-168.2	6.4	Yes
12.	Thr149-Gly152	TSGG	I	-59.3	-27.8	53.8	-81.8	0.8	-59.7	5.2	No
13.	Asp158-Leu161	DFGL	II	-79.2	150.6	58.8	71.3	15.8	-	6.5	No
14.	Leu178-Arg181	LWYR	I	-64.8	-26.7	-56.3	-110.3	0.9	-49.1	5.4	No
15.	Pro212-Cys215	PLFC	VIII	-63.7	-44.9	-177.4	-130.6	111.1	-56.3	6.3	Yes
16.	Pro239-Val242	PRDV	IV	-71.9	-39.0	-63.8	-106.9	56.8	-57.8	6.4	Yes
17.	Val242-Pro245	VSLP	VIII	-72.6	-22.5	53.4	-106.6	110.4	-163.2	6.8	Yes
18.	Ser259-Pro262	SVVP	IV	-119.8	-19.3	-68.0	-132.0	77.2	-164.9	6.1	Yes
19.	Val261-Met264	VPEM	I	-62.9	-24.8	-24.7	-84.9	-7.3	-64.1	5.7	No
20	Asn279-Lys282	NPHK	I	-65.8	-22.7	24.1	-78.7	-16.4	-57.7	5.5	No
21.	Pro280-Arg283	PHKR	I	-78.7	-16.4	-57.7	-105.1	-5.8	-63.5	5.0	Yes
22.	His292-Leu295	HSYL	IV	-56.8	-29.9	49.6	-57.8	-36.4	-179.3	5.7	No
23.	Ser293-His296	SYLH	I	-57.8	-36.4	-179.3	-101.1	-11.9	-66.2	5.1	Yes

Number of beta turns in chain A: 23

* Asterisked motifs correspond to those illustrated in the motif plots at the top of the page.

* Residue colouring corresponds to the colouring given in the motif plots and in the RasMol displays.

Table 6: Gamma turns.

Sl. No.	Start	End	Sequences	Turn Type	Residue i+1			i to i+2 CA-dist
					Phi	Psi	Chi1	
1.	Thr172	Val174	TPV	INVERSE	-74.3	90.0	25.7	5.7
2.	Asp298	Gly300	DEG	INVERSE	-62.3	94.0	-71.5	5.3

cryo-EM) could be used to gain deeper insights into the dynamics and biological functions in the future.

CONCLUSION

We aimed to correlate sequence properties with structural organization in a 303 amino acid protein: this study reveals that sequence features, such as the protein's glycine and Proline content, contribute to the protein's stability and flexibility, with glycine and proline favoring turns and local conformational changes. A secondary-structure analysis reveals that the structure is highly ordered and consists of several α-helices and β-strands with loops and turns that facilitate reversals in the chain and optimal long-range packing, respectively. The quality of the structure is also good, as assessed by model reliability, with the majority of the residues situated in favourable Ramachandran regions, and the supporting G-factor parameters that suggest appropriate conformations of the backbone and dihedral angles, and covalent geometries. Overall, the available evidence indicates that the globular protein is well folded and robust and gives a good platform for further functional and interaction studies.

ACKNOWLEDGEMENT

The author would like to thank the Department of Laboratory Medicine at Al-Baha University for providing the necessary facilities to conduct this research.

ABBREVIATIONS

AI: Artificial Intelligence; **Cα:** Alpha Carbon; **CDK4:** Cyclin-Dependent Kinase 4; **Cryo-EM:** Cryogenic Electron Microscopy; **FASTA:** Fast-All sequence format; **G-factor:** Geometric Factor; **G1-S:** Gap 1 to Synthesis phase; **ProtScale:** Protein Scale; **X-ray:** X-ray Crystallography; **3D:** Three-Dimensional; **Å:** Ångstrom; **φ:** Phi; **ψ:** Psi; **χ:** Chi.

CONFLICT OF INTEREST

The authors declare that there is no conflict of interest.

FUNDING

This work was supported by the Department of Laboratory Medicine, Faculty of Applied College, Al-Baha University, Saudi Arabia.

REFERENCES

Branden, C., & Tooze, J. (1999). Introduction to protein structure (2nd ed.). Garland Publishing.

Chen, L., Li, Q., Nasif, K. F. A., Xie, Y., Deng, B., Niu, S., Pouriyeh, S., Dai, Z., Chen, J., & Xie, C. Y. (2024). AI-driven deep learning techniques in protein structure prediction. International Journal of Molecular Sciences, 25(15), 8426.

Chou, P. Y., & Fasman, G. D. (1974). Prediction of protein conformation. Biochemistry, 13(2), 222-245.

De Brevern, A. G. (2016). Extension of the classical classification of β-turns. Scientific Reports, 6(1), 33191.

De Santis, F., Miotto, M., Di Rienzo, L., *et al.* (2022). Spatial organization of hydrophobic and charged residues affects protein thermal stability and binding affinity. Scientific Reports, 12(1), 12087.

Dill, K. A., & MacCallum, J. L. (2012). The protein-folding problem, 50 years on. Science, 338(6110), 1042-1046.

Engh, R. A., & Huber, R. (1991). Accurate bond and angle parameters for X-ray protein structure refinement. Acta Crystallographica Section A, 47(4), 392-400.

Gasteiger, E., Hoogland, C., Gattiker, A., *et al.* (2005). Protein identification and analysis tools on the ExPASy server. In J. M. Walker (Ed.),The proteomics protocols handbook (pp. 571-607). Humana Press.

Giménez-Andrés, M., Čopič, A., & Antonny, B. (2018). The many faces of amphipathic helices. Biomolecules, 8(3), 45.

Ho, B. K., Thomas, A., & Brasseur, R. (2003). Revisiting the Ramachandran plot: Hard-sphere repulsion, electrostatics, and H-bonding in the alpha-helix. Protein Science, 12(11), 2508-2522.

Hou, J., Sims, G. E., Zhang, C., & Kim, S. (2003). A Global Representation of the protein fold space. Proceedings of the National Academy of Sciences of the United States of America, 100(5), 2386-2390.

Hutchinson, E. G., & Thornton, J. M. (1994). A revised set of potentials for beta-turn formation in proteins. Protein Science, 3(12), 2207-2216.

Imai, K., & Mitaku, S. (2005). Mechanisms of secondary structure breakers in soluble proteins. Biophysics (Nagoya-shi), 1, 55-65.

Jones, D. T. (1999). Protein secondary structure prediction based on position-specific scoring matrices. Journal of Molecular Biology, 292(2), 195-202.

Jumper, J., Evans, R., Pritzel, A., *et al.* (2021). Highly accurate protein structure prediction with AlphaFold. Nature, 596(7873), 583-589.

Kyte, J., & Doolittle, R. F. (1982). A simple method for displaying the hydropathic character of a protein. Journal of Molecular Biology, 157(1), 105-132.

Laskowski, R. A., MacArthur, M. W., Moss, D. S., & Thornton, J. M. (1993). PROCHECK: A program to check the stereochemical quality of protein structures. Journal of Applied Crystallography, 26(2), 283-291.

Lovell, S. C., Davis, I. W., Arendall, W. B., *et al.* (2003). Structure validation by Cα geometry: ϕ, ψ and Cβ deviation. Proteins: Structure, Function, and Bioinformatics, 50(3), 437-450.

Morris, R., Black, K. A., & Stollar, E. J. (2022). Uncovering protein function: From classification to complexes. Essays in Biochemistry, 66(3), 255-285.

Perczel, A., & Hollósi, M. (1996). Turns. In G. D. Fasman (Ed.),Circular dichroism and the conformational analysis of biomolecules (pp. 285-380). Springer.

Ramachandran, G. N., Ramakrishnan, C., & Sasisekharan, V. (1963). Stereochemistry of polypeptide chain configurations. Journal of Molecular Biology, 7, 95-99.

Richardson, J. S., & Richardson, D. C. (2002). Natural beta-sheet proteins use negative design to avoid edge-to-edge aggregation. Proceedings of the National Academy of Sciences of the United States of America, 99(5), 2754-2759.

Schlick, T. (2010). Protein structure hierarchy. In Molecular modeling and simulation: An interdisciplinary guide (pp. 105-128). Springer.

Skrbic, T., Giacometti, A., Hoang, T. X., Maritan, A., & Banavar, J. R. (2024). Amino-acid characteristics in protein native state structures. Biomolecules, 14(7), 805.

Thornton, J. M., Laskowski, R. A., & Borkakoti, N. (2021). AlphaFold heralds a data-driven revolution in biology and medicine. Nature Medicine, 27(10), 1666-1669.

Tsuboyama, K., Dauparas, J., Chen, J., *et al.* (2023). Mega-scale experimental analysis of protein folding stability in biology and design. Nature, 620(7973), 434-444.

Wang, H., Logan, D. T., Danielsson, J., & Oliveberg, M. (2020). Exposing the distinctive modular behavior of β-strands and α-helices in folded proteins. Proceedings of the National Academy of Sciences of the United States of America, 117(46), 28775-28783.

Yasuda, T., Morita, R., Shigeta, Y., & Harada, R. (2022). Structural validation by the G-factor properly regulates boost potentials imposed in conformational sampling of proteins. Journal of Chemical Information and Modeling, 62(14), 3442-3452.

Zhao, B., Basu, S., & Kurgan, L. (2025). DescribePROT database of residue-level protein structure and function annotations. In Methods in Molecular Biology (Vol. 2867,169-184). Springer.

Cite this article: Alghamdi RM. Structural and Conformational Landscape of CDK4: The Basis for Next-Generation Kinase Therapeutics. J Young Pharm. 2026;18(3):840-9.